JOURNAL OF AGRICULTURAL AND FOOD CHEMISTRY

Article

Isolation, structural elucidation, and LC-MS analysis of steroidal glycosides from Polygonatum odoratum

Qingbo Liu, Wei Li, Kazuya Nagata, Hongwei Fu, Shunpei Okada, Ikumi Tanabe, Yumi Kobori, Koji Higai, Wada Norie, Tatsunori Sasaki, Yoshihisa Asada, Huanxin Zhao, Hong Bai, and Kazuo Koike

J. Agric. Food Chem., **Just Accepted Manuscript** • DOI: 10.1021/acs.jafc.7b04488 • Publication Date (Web): 20 Dec 2017

Isolation, structural elucidation, and LC-MS analysis of steroidal glycosides from *Polygonatum odoratum*

Qingbo Liu,[†] Wei Li,[†,*] Kazuya Nagata,[†] Hongwei Fu,[‡,*] Shunpei Okada,[†] Ikumi Tanabe,[†] Yumi Kobori,[†] Koji Higai,[†] Wada Norie,[†] Tatsunori Sasaki,[†] Yoshihisa Asada,[†] Huanxin Zhao,[§] Hong Bai,[#] Kazuo Koike[†]

[†]*Faculty of Pharmaceutical Sciences, Toho University, Miyama 2-2-1, Funabashi, Chiba 274-8510, Japan*

[‡]*Zhejiang University Technology Transfer Center, Industrial Technology Research Institute of Zhejiang University, Hangzhou, Zhejiang Province, 310058, P. R. China*

[§]*Institute of Materia Medica, Shandong Academy of Medical Sciences, Jinan, Shandong 250062, P. R. China*

[#]*College of Life Science and Technology, Huazhong University of Science and Technology, Wuhan, Hubei 430074, P. R. China*

ABSTRACT

The rhizomes of *Polygonatum odoratum* represent a traditional Chinese medicine and functional food. A phytochemical investigation resulted in the isolation of eight steroidal glycosides (**1-8**), including two new compounds, polygonatumosides F (**1**) and G (**2**). The structures were elucidated by spectroscopic data and chemical reactions. Compound **7** showed anti-proliferation activity against human hepatocellular carcinoma cell line HepG2 (IC_{50} 3.2 μM). The chemical profile and contents of steroidal glycosides of *P. odoratum* rhizomes collected at different dates and geographical locations were also investigated, indicating that the rational harvest of *P. odoratum* in spring and autumn is preferable to obtain higher levels of steroidal glycosides. Compounds **1** and **7** showed the highest contents in all *P. odoratum* samples, and have potential to serve as chemotaxonomic and chemical markers for quality control of this important plant material. 14-Hydroxylation may be a key step for the biosynthesis of **1-7**.

KEYWORDS: *Polygonatum odoratum*, *steroidal glycosides*, *structural elucidation*, *anti-proliferation activity, LC-MS analysis*

INTRODUCTION

Polygonatum odoratum (Mill.) Druce (Angular Solomon's seal), belonging to the Liliaceae family, is a perennial herbaceous plant widely distributed in East Asia and Europe. The edible rhizomes of *P. odoratum,* known as "Yu Zhu" in China, are used in functional foods and healthy tea products,[1] and in traditional Chinese medicine for treating hypoimmunity, rheumatic heart disease and diabetes.[2] Biological investigations of the extract from *P. odoratum* have demonstrated various bioactive effects, such as antioxidant, anti-diabetes and anti-tumor effects.[3-5] These biological functions are also closely related to the characteristic chemical constituents, including steroidal glycosides and homoisoflavonoids.[5-7] Our previous phytochemical investigation of the rhizomes of *P. odoratum* reported the isolation and structural elucidation of homoisoflavonoids and dihydrochalcones, which showed activation effects on adenosine monophosphate activated protein kinase (AMPK),[8] as well as cholestane-type and spirostane-type steroidal glycosides, which showed antifungal activity against *Candida albicans* JCM1542 and *Aspergillus fumigatus* JCM1738.[9]

In a further investigation, we found that, in the cultivated *P. odoratum*, the rhizomes contained steroidal glycosides which have not been isolated in our previous study. Therefore, a comprehensive re-investigation of the steroidal glycosides in the rhizomes of cultivated *P. odoratum* was carried out. As a result, eight steroidal glycosides (**1-8**), including two new compounds (**1** and **2**), were isolated and structurally elucidated. The anti-proliferative activity was evaluated against human hepatocellular carcinoma cell line HepG2. Furthermore, an LC-ESI-MS analysis was performed to better understanding of the profile and contents of the steroidal glycosides in the rhizomes of *P. odoratum*. On the basis of summarized MS fragmentation of isolated steroidal glycosides, a simple LC-ESI-MS method was established via a combination of selected ion monitoring (SIM) and full scan modes, which was applied to the analysis of plant samples from different collection dates and different areas. A biogenesis pathway of these steroidal glycosides was also proposed.

MATERIALS AND METHODS

Instrumentation and Reagents. A JASCO P-2200 polarimeter was used to measure optical rotations in a 0.5-dm cell. A JASCO FT/IR-4100 Fourier transform infrared spectrometer was used to measure the IR spectra by the KBr disk method. A JEOL ECA-500 spectrometer was used to measure the ^{1}H and ^{13}C NMR spectra, and the measuring deuterated solvent was used as the internal reference, and the chemical shifts are in δ (ppm). A JEOL JMS-700 MStation was used to measure HRFABMS.

Diaion HP-20 (Mitsubishi Chemical Corporation, Tokyo, Japan) and ODS (100-200 mesh, Chromatorex DM1020T ODS, Fuji Silysia Chemical Co., Ltd., Aichi, Japan) were used for column chromatography. MPLC separation was carried out on an AI-580 System (Yamazen, Japan) using an ODS column (400 × 40 mm). Semi-preparative HPLC was carried out on a Waters 600E (MILLIPORE) HPLC pump equipped with a SPD-10A (SHIMADZU) intelligent UV/VIS detector and a Shodex RI-72 Differential Refractometer detector. A RP-C18 silica gel column (YMC Actus Triart C18, 250 × 20 mm) was used at a flow rate of 5.0 mL/min. HPLC-grade methanol and 1,4-dioxane were from Wako Pure Chemical Industries, Ltd. (Osaka, Japan), and HPLC-grade acetonitrile was from Kanto Chemical Co., Inc. (Tokyo, Japan). Water was purified using a Milli-Q water purification system (Millipore, USA).

LC-MS analysis was performed with an LCMS-8040 Triple Quadrupole LC/MS/MS Mass Spectrometer (Shimadzu Co., Ltd., Kyoto, Japan) consisting of a LC-20AD solvent delivery pump, SIL-20AC autosampler, CTO-20A Oven, SPD-20A detector, CBM-20A controller and electrospray ionization source. LC-MS grade acetonitrile, ethanol, formic acid, and water were from Wako Pure Chemical Industries, Ltd.

Plant Material. The rhizomes of *P. odoratum* used for the phytochemical investigation were cultivated for three years in a farm, at Wuhu City of Anhui province, P. R. China (31º33′ N, 118º38′ E) and were collected in November 2014.

For the LC-MS analysis, the plant materials were cultivated in the same place as those for the

phytochemical investigation, and were monthly collected from April 2015-June 2017 (except for January, February, and October 2016). After collection, the rhizomes of these plant materials were cut and freeze-dried. Similarly, a wild *P. odoratum* and two cultivars were collected from Anhui, Liaoning and Hunan provinces, P. R. China, respectively (Table 2).

All plant materials were identified by Prof. Lin Zhang, (Zhejiang University, P. R. China). The voucher specimens (Table 2) were deposited in the Department of Pharmacognosy, Faculty of Pharmaceutical Sciences, Toho University, Japan.

Extraction and Isolation. The dried rhizomes of *P. odoratum* (1 kg) were cut into small pieces and pulverized into a coarse powder. The dried powder was ultrasonically extracted with 70% aqueous EtOH at room temperature for 2 h, 3 times. The extract liquid was combined and concentrated under reduced pressure to give the extract (506 g). A part of the extract (323 g) was partitioned between *n*-BuOH and H_2O. The *n*-BuOH fraction (60 g) was subjected to Diaion HP-20 column chromatography and eluted with gradients of H_2O, MeOH and acetone. The MeOH eluate fraction was further separated by MPLC with a gradient of MeOH-H_2O (from 1:9 to 10:0, v/v) to yield ten sub-fractions (Fr.1-Fr.10). Further separation was achieved by semi-preparative RP-HPLC. Namely, compounds **1** (260 mg) and **8** (42 mg) were isolated from Fr.4 (0.69 g) using dioxane-H_2O (42:58, v/v), compounds **2** (38 mg) and **3** (52 mg) from Fr.5 (0.48 g) using dioxane-H_2O (44:56, v/v), compounds **5** (76 mg) and **6** (36 mg) from Fr.7 (0.38 g) using dioxane-H_2O (57:43, v/v), and compounds **4** (3 mg) and **7** (141 mg) from Fr.8 (1.1 g) with MeCN-H_2O (45:55, v/v).

*Polygonatumoside F (**1**)*: amorphous powder, $[\alpha]_D^{21}$ -52.0 (*c* 0.3, pyridine); IR (KBr) max: 3408, 2930, 1717, 1371, 1256, 1159, 1077, 1038, 870 cm^{-1}; ^1H NMR (pyridine-d_5, 500 MHz) and ^{13}C NMR (pyridine-d_5, 125 MHz), see Table 1; positive-ion HRFABMS *m/z* 1211.5695 $[M\text{-}H_2O+H]^+$ (calcd for $C_{56}H_{91}O_{28}$, 1211.5697).

*Polygonatumoside G (**2**)*: amorphous powder, $[\alpha]_D^{21}$ -45.4 (*c* 0.2, pyridine); IR (KBr) max: 3392, 2931, 1717, 1456, 1379, 1270, 1159, 1098, 1032, 908 cm^{-1}; ^1H NMR (pyridine-d_5, 500 MHz) and ^{13}C

NMR (pyridine-d_5, 125 MHz), see Table 1; positive-ion HRFABMS *m/z* 593.3690 $[M\text{-}H_2O+H]^+$ (calcd for $C_{33}H_{53}O_9$, 593.3690).

Acid Hydrolysis of Compounds 1 and 2. Compounds **1** (1 mg) and **2** (1 mg) were separately dissolved in 1 M HCl (dioxane-H_2O, 1:1, 25 mL) and heated at 100 ºC for 2 h. After the dioxane was removed by evaporation, the solution was partitioned between EtOAc and H_2O. Evaporation of the aqueous layer afforded the sugar fraction. After dissolved in H_2O (1 mL), a solution of (*S*)-(-)-1-phenylethylamine (3 μL) and $NaBH_3CN$ (2 mg) in EtOH (1 mL) was added, and incubated at 40 ºC overnight. Then, glacial AcOH (0.2 mL) was added, and the reaction mixture was evaporated to dryness. Ac_2O (50 μL) and DMAP (2.0 mg) in pyridine (2 mL) were added for 24 h at room temperature. The reaction mixture was evaporated, and chromatographed on a Sep-Pak C18 cartridge (Waters, USA) with CH_3CN-H_2O (1:4 and 1:1, v/v, each 10 mL). The CH_3CN-H_2O (1:1, v/v) eluate consisting a mixture of 1-[(*S*)-*N*-acetyl-methylbenzylamino]-1-deoxy-alditol acetate derivatives of monosaccharides, was analyzed by LC-MS. Column, YMC Triart C18 (3.0 μm, 150 × 20 mm); solvent, CH_3CN-H_2O (35:65, v/v); flow rate, 0.2 mL/min; column temperature, 35 °C. Derivatives of D-xylose, D-galactose, and D-glucose were detected at t_R (min) of 18.2 (D-xylose), 21.4 (D-galactose), and 26.8 (D-glucose).

LC-MS Analysis. Pretreatment of the plant samples for LC-MS analysis was as follows: fine powder of the plant materials (1 g, accurately weighed) was ultrasonically extracted with 70% EtOH (20 mL) for 1 h. After centrifugation at 3000 rpm for 10 min, the supernatant was filtered through a 0.45 μm syringe filter. A volume of 2 μL was injected for LC-MS analysis.

The ESI parameters for LC-MS analysis were: interface voltage, 4.5 kV in the positive ion mode and -3.5 kV in the negative ion mode; collision voltage, 15 V; dry gas, 15 L/min; dry temperature, 350 °C. For qualitative analysis, total ion current (TIC) modality were acquired in the positive and negative-ion modes from *m/z* 100 to 1600, and characteristic fragment ions (*m/z* 593, 395, 577, 415 and 399) in positive SIM mode were checked. For quantitative purpose, in negative

SIM mode on the ESI generated most abundant ion, corresponding to the pseudo-molecular ion $[M-H]^-$ or $[M+HCOO]^-$, for each steroidal glycosides; *m/z* 1227 $[M-H]^-$ for **1**, *m/z* 655 $[M+HCOO]^-$ for **2**, *m/z* 1211 $[M-H]^-$ for **3**, *m/z* 639 $[M+HCOO]^-$ for **4**, *m/z* 1047 $[M-H]^-$ for **5**, *m/z* 915 $[M-H]^-$ for **6**, *m/z* 1031 $[M-H]^-$ for **7** and *m/z* 787 $[M+HCOO]^-$ for **8**.

HPLC was performed on a YMC-Triart C_{18} (3.0 μm, 150 × 20 mm) at 35 °C. The mobile phase was composed of A (0.1% formic acid in H_2O) and B (acetonitrile) with a gradient elution: 0-40 min, 10%-100% B; 40-50 min, 100% B. The column was equilibrated for 20 min under the initial conditions. The flow rate was 0.2 mL/min.

WST-1 Cell Proliferation Assay. Human hepatocellular carcinoma cell line HepG2 cells were seeded on 96-well culture plates (100 μL per well, 20×10^4 cell/mL) and incubated for 6 h at 37 °C. Then, the cells were exposed to different concentrations of compounds for 48 h. The number of living cells was measured by a Premix WST-1 Cell Proliferation Assay System (TaKaRa, Shiga, Japan), according to the manufacturer's instructions. Epirubicin was used as the positive control.

Results and Discussion

Isolation and Structural Elucidation. Eight steroidal glycosides were isolated after multiple chromatographic procedures of the *n*-BuOH soluble fraction from the 70% EtOH extract of the dried rhizomes of *P. odoratum*. Based on the comparison with the NMR and MS data previously reported in the literature, known compounds (**3-8**) were identified as timosaponin H1 (**3**),[10] (25*S*)-funkioside B (**4**),[11] (25*S*)-(3*β*,14*α*)-dihydroxy-spirost-5-ene-3-*O*-*β*-D-glucopyranosyl-(1→2)-[*β*-D-xylopyranosyl-(1→3)]-*β*-D-glucopyranosyl-(1→4)-*β*-D-galacopyranoside (**5**),[12] (25*S*)-(3*β*,14*α*)-dihydroxy-spirost-5-en-3-*O*-*β*-D-glucopyranosyl-(1→2)-*β*-D-glucopyranosyl-(1→4)-*β*-D-galactopyranoside (**6**),[9] 3-*O*-*β*-D-glucopyranosyl-(1→2)-[*β*-D-xylopyranosyl-(1→3)]-*β*-D-glucopyranosyl-(1→4)-*β*-D-galaco pyranosyl-yamogenin (**7**),[13] and

(22*S*)-cholest-5-ene-1*β*,3*β*,16*β*,22-tetrol-1-*O*-*α*-L-rhamnopyranosyl-16-*O*-*β*-D-glucopyranoside (**8**).[14] Among them, compounds **3** and **4** were obtained from the genus of *Polygonatum* for the first time. Compounds **1** and **2** were unreported steroidal glycosides, and their structures were elucidated as follows.

Compound **1** was obtained as a white amorphous powder. The molecular formula was assigned as $C_{56}H_{92}O_{29}$ on the basis of the positive-ion HRFABMS peak at *m/z* 1211.5695 $[M\text{-}H_2O+H]^+$ (calcd for $C_{56}H_{91}O_{28}$, 1211.5697), together with its NMR data (Table 1). The ^{1}H NMR spectrum of **1** exhibited two typical methyl singlets at δ_H 0.98 (s, CH_3-19) and 1.10 (s, CH_3-18), two methyl doublets at δ_H 1.04 (d, J = 6.5 Hz, CH_3-27) and 1.32 (d, J = 6.9 Hz, CH_3-21), two oxymethylene proton resonances at δ_H 4.07 (H-26a) and 3.50 (dd, J = 9.5, 6.9 Hz, H-26b), and the olefinic proton resonance at δ_H 5.36 (H-6). The above ^{1}H NMR data, together with the characteristic carbon resonances related to a hemiketalic carbon at δ_C 111.0 (C-22) and two olefinic carbons at δ_C 140.6 (C-5) and 122.2 (C-6), suggested **1** to have a $\Delta^{5,6}$-furostanol skeleton. Furthermore, the NMR spectroscopic data attributed to the aglycone of **1** were similar to those of **3**. However, in comparison to **3**, C-14 was shifted downfield (δ_C 86.4) indicating a hydroxyl substituent in this position. The configuration of the substituent at C-14 was determined by the correlations observed in the ROESY spectrum (Figure 2). Namely, the key ROESY correlations between H-16/H-17, CH_3-18/H-15b (δ_H 1.85), and H-16/H-15a (δ_H 2.27), suggested *α*-orientation of the 14-hydroxyl group. The *α*-configuration of the C-22 hydroxyl group was deduced from the hemiketalic carbon resonance at δ_C 111.0, compared to that for the *β*-configuration at δ_C 115.0.[15] Further ROESY correlations between the H-20/H-23 unambiguously determined the *α*-configuration of the C-22 hydroxyl group. The 25*S* configuration was inferred by the proton chemical shift difference between the geminal protons H-26a and H-26b (*Δ*ab = 0.57): *δ*ab ≥ 0.57 ppm for 25*S* and *δ*ab ≤ 0.48 ppm for 25*R*, when in pyridine-d_5.[16] For the sugar moiety, the ^{1}H and ^{13}C NMR spectra of **1** revealed resonances that were assigned to three *β*-glucopyranosyl (Glc), one *β*-galactopyranosyl (Gal), and one *β*-xylopyranosyl

(Xyl) moieties. The corresponding anomeric carbons were observed at δ_C 105.1, 105.0, 104.8, 102.8, and 104.9, and the corresponding anomeric proton resonances at δ_H 4.79 (d, J = 7.7 Hz, Glc3-H-1), 5.13 (d, J = 8.1 Hz, Glc1-H-1), 5.53 (d, J = 7.7 Hz, Glc2-H-1), 4.83 (d, J = 7.5 Hz, Gal-H-1), and 5.20 (d, J = 7.7 Hz, Xyl-H-1), respectively. Upon acid hydrolysis of **1** with 1 M HCl in dioxane-H_2O, the component sugar composition was determined to be a combination of D-glucose, D-xylose and D-galactose on the basis of LC-MS analysis of their 1-[(*S*)-*N*-acetyl-methylbenzylamino]-1-deoxy-alditol acetate derivatives. The sequence and linkage sites of the sugar chain were deduced from the glycosylation shifted ^{13}C resonances for C-3 (δ_C 78.3), C-26 (δ_C 75.4), Gal-C-4 (δ_C 79.8), Glc1-C-2 (δ_C 81.3) and Glc1-C-3 (δ_C 86.9), as well as from the HMBC data (Figure 1). Namely, the key HMBC correlations (Figure 1) between Gal-H-1 (δ_H 4.83) and C-3 (δ_C 78.3), Glc1-H-1 (δ_H 5.13) and Gal-C-4 (δ_C 79.8) of, Glc2-H-1 (δ_H 5.53) and Glc1-C-2 (δ_C 81.3), and Xyl-H-1 (δ_H 5.20) and Glc1-C-3 (δ_C 86.9), suggested a sequence of the tetrasaccharide chain at C-3. Similarly, the HMBC correlation between Glc3-H-1 (δ_H 4.79) and C-26 (δ_C 75.4) indicated that a *β*-D-glucopyranosyl moiety was located at the C-26. Thus, the structure of **1** was determined to be (25*S*)-26-*O*-(*β*-D-glucopyranosyl)-furost-5-ene-3*β*,14*α*,22*α*,26-tetrol 3-*O*-*β*-D-glucopyranosyl-(1→2)-[*β*-D-xylopyranosyl-(1→3)]-*β*-D-glucopyranosyl-(1→4)-*β*-D-galacto pyranoside, and named polygonatumoside F.

Compound **2** was isolated as a white amorphous powder, $[\alpha]_D^{21}$ -45.4 (*c* 0.2, pyridine). The molecular formula was inferred as $C_{33}H_{54}O_{10}$ according to the positive-ion HRFABMS peak at *m/z* 593.3690 $[M-H_2O+H]^+$ (calcd for $C_{33}H_{53}O_9$, 593.3690). The NMR spectra of compound **2** were very similar to that of **1** except in those regions of the spectra derived from the sugars, suggesting that **2** has the same aglycone skeleton with **1** but with differences in sugar parts. The ^1H NMR data revealed the presence of only one *β*-glucopyranosyl moiety with anomeric proton at δ_H 4.79 (1H, d, J = 7.7 Hz), which was determined to be the D-form by LC-MS analysis after acid hydrolysis and chemical derivatization. An upfield chemical shift was observed for C-3 (from δ_C 78.3 in **1** to δ_C 71.3

in **2**), suggesting the presence of a free secondary hydroxyl group at C-3 of **2**, whereas the 10-ppm downfield shift observed for C-26 (δ_C 75.4) relative to a free primary hydroxyl group indicated glycosylation at this position, which was further evidenced by the HMBC correlation from Glc-H-1 (δ_H 4.79) to C-26 (δ_C 75.4) (Figure 1). Thus, the structure of **2** was established as (25*S*)-furost-5-ene-3β,14α,22α,26-tetrol 26-*O*-β-D-glucopyranoside, and named polygonatumoside G.

Anti-proliferation Activity against HepG2 Cell. Since *P. odoratum* extract[4] and structural similar steroidal glycosides[17,18] have been reported anti-proliferation activities against human cancer cells, all isolated compounds (**1**-**8**) were evaluated for their anti-proliferation activities against HepG2 cell by WST-1 assay. Compound **7** significantly reduced the viability of HepG2 cell (IC_{50}, 3.2 μM), which was comparable to the positive control epirubicin (IC_{50}, 1.6 μM). Other seven compounds appeared to show no cytotoxicity against this cell line (IC_{50} > 20 μM). Comparison with the structures of **1-8**, steroidal glycosides possessing a $\Delta^{5,6}$-spriostanol skeleton without 14α-hydroxyl group exhibited significant anti-proliferation activity. The result was in agreement with a previous report by Yu et al, which showed that a series of similar characteristic steroidal glycosides exhibited cytotoxicity against a variety of human cancer cell lines.[17] Despite that homoisoflavonoids[7] and lectin[19] from *P. odoratum* have been reported cytotoxicity against human cancer cell lines, to our best knowledge, this is the first report of identification of an anti-proliferative steroidal glycoside from *P. odoratum*.

ESI-MS Fragmentation Pattern of Isolated Steroidal Glycosides. ESI-MS spectra were obtained in both positive- and negative-ion modes by LC-MS analysis. Due to more ion fragment information, the fragmentation behaviors of compounds **1-8** were analyzed and summarized in positive mode. As shown in Figure 3, the furostane-type glycosides (**1-4**) readily generated an $[M\text{-}H_2O+H]^+$ ion via cleavage of the hydroxyl group occurring at the C-22 position, which was different from spirostane-type steroidal glycosides (**5-7**). When furostane- and spirostane-type steroidal glycosides

(**1**, **2**, **5** and **6**) were substituted with a hydroxyl group at their C-14 position, the main fragment ions at *m/z* 593 and/or 395 were usually generated. On the other hand, if the fragment ions at *m/z* 577 and/or 415 were detected, there should be no hydroxyl substituent at C-14 position of aglycone (**3**, **4** and **7**). Compounds **1**, **3**, **5** and **7** were selected as suitable representative samples to summary the proposed fragmentation pathway of furostane- and spirostane-type steroidal glycosides, as shown in Figure 4. For cholestane glycoside **8**, it easily produced a base peak at *m/z* 399 [aglycone-$2H_2O$+H]$^+$.

LC-MS Analysis of *P. odoratum* Extract. On the basis of fragmentation pathway of compounds **1-8**, an LC-MS analysis method was established to profile the extract of *P. odoratum*. MS scan in both positive- and negative-ion modes provided valuable information for structural identification on the basis of the aforementioned ESI-fragmentation analysis. The full scan combining with positive SIM channels (*m/z* 593, 395, 577, 415 and 399) profiled the steroidal glycosides from *P. odoratum.* Simultaneously, negative SIM scan was selected for the quantitative analysis for the eight steroidal glycosides (**1-8**). As shown in Figure 5, all the isolated steroidal glycosides (**1-8**) were detectable, and **1** and **7** showed the highest contents in the crude extract of *P. odoratum*, which were in agreement with phytochemical investigation results.

LC-MS Analysis of *P. odoratum* Samples Collected from Different Dates and Geographical Locations. In order to investigate the influence of collection dates on the chemical profile and contents of steroidal glycosides, the cultivated *P. odoratum* samples were monthly collected from April 2015 to June 2017 (Table 2), and the these samples were analyzed by established LC-MS method. The total contents of steroidal glycosides were in the range of 6.6-15.2 mg/g dry weight with considerable variation among the samples of different collection dates. As shown in Figure 6, the total contents of steroidal glycosides in spring and autumn were higher than that in summer and winter. Considering that steroidal glycosides are the main active ingredients of *P. odoratum*, this result is in good agreement with the fact that the rhizomes of *P. odoratum* harvested in spring and autumn is considered as the premium materials for usage of medicine and function foods in China.[20]

Comparative analysis of the steroidal glycosides of wild and cultivated *P. odoratum* from different geographical locations was also carried out. The contents and composition of steroidal glycosides were similar in the cultivated and wild *P. odoratum* from Anhui province, but were significantly different from those of cultivars in Liaoning and Hunan provinces. Among the eight steroidal glycosides, compounds **1** and **7** were the main constituents, and they accounted for approximately 70% of the total steroidal glycosides contents and could be easily observed in the LC-MS chromatogram. Therefore, compounds **1** and **7** have potential to serve as chemotaxonomic and chemical markers for quality control of this important plant material. In addition, steroidal glycosides in the fruits and leaves were also investigated, and those steroidal glycosides in the rhizomes were not detectable in the fruits and leaves.

Biosynthetic Pathway of Steroidal Glycosides 1-8. Steroidal glycosides (**1-8**) share a common biosynthetic precursor, (22*S*)-cholest-5-ene-3*β*,16*β*,22-triol (**10**). C-1 hydroxylation, followed by C-1, C-16 glucosylation of the precursor **10**, produce cholestane-type glycoside **8**. Furostane-type steroidal glycosides (**1-4**) and spirostane-type steroidal glycosides (**5-7**) were produced by a series of biosynthetic reactions including oxidation, glycosylation, and deglucosylation from **10**, as shown in Figure 7. The aforementioned LC-MS analysis of steroidal glycosides in *P. odoratum* resulted that **1** (furostane-type with 14-OH) and **7** (spirostane-type without 14-OH) represented two major compounds in the biosynthesis routes divided by 14-hydroxylation of 16,26-dihydroxy-22-keto-cholesterol (**12**), which may be a key step for the biosynthesis of **1-7**.

ACKNOWLEDGMENTS

The authors are grateful to Mr. Yonghui Wang (President of Anhui Lianzhe Yuzhu Co. Ltd., P. R. China) for providing plant materials of cultivated *P. odoratum*.

Supporting Information. The Supporting Information is available free of charge on the ACS Publications website.

IR, NMR, HRFABMS spectra of compounds **1** and **2** (PDF)

AUTHOR INFORMATION

Corresponding Authors:

* Tel.: +81-47-4721161. Fax: +81-47-4721404. E-mail: liwei@phar.toho-u.ac.jp (W. Li); Tel.: +86 571 88206950. Fax: +86-571-88981185. E-mail: fhw668@zju.edu.cn (H. Fu)

ORCID

Wei Li: 0000-0003-4143-8597

Notes

The authors declare no competing financial interest.

REFERENCES

(1) Yang, L. S.; Liu, D. T.; Yang, K. J. Dietary Treatment of Chinese Medicine. Jilin People's Publishing House, Changchun, **1991**, pp. 62-63.

(2) Yu, C. A Dictionary of the Traditional Chinese Medicine. Beijing: Chinese Medical Science Press, **1993**, *Vol. 1*, pp 1331.

(3) Wang, D.; Zeng, L.; Li, D.; Pu, W. Antioxidant activities of different extracts and homoisoflavanones isolated from the *Polygonatum odoratum*. *Nat. Prod. Res.* **2013**, *27*, 1111-1114.

(4) Tai, Y.; Sun, Y. M.; Zou, X.; Pan, Q.; Lan Y. D.; Huo, Q.; Zhu, J. W.; Guo, F.; Zheng, C. Q.; Wu C. Z.; Liu, H. Effect of *Polygonatum odoratum* extract on human breast cancer MDA-MB-231 cell proliferation and apoptosis. *Exp. Ther. Med.* **2016**, *12*, 2681-2687.

(5) Zhou, X.; Liang, J.; Zhang, Y.; Zhao, H.; Guo, Y.; Shi, S. Separation and purification of α-glucosidase inhibitors from *Polygonatum odoratum* by stepwise high-speed counter-current chromatography combined with Sephadex LH-20 chromatography target-guided by ultrafiltration-HPLC screening. *J. Chromatogr. B* **2015**, *985*, 149-154.

(6) Choi, S. B.; Park, S. A steroidal glycoside from *Polygonatum odoratum* (Mill.) Druce. improves insulin resistance but does not alter insulin secretion in 90% pancreatectomized rats. *Biosci. Biotechnol. Biochem.* **2002**, *66*, 2036-2043.

(7) Rafi, M. M.; Vastano, B. C. Identification of a structure specific Bcl-2 phosphorylating homoisoflavone molecule from Vietnamese coriander (*Polygonatum odoratum*) that induces apoptosis and G2/M cell cycle arrest in breast cancer cell lines. *Food Chem*. **2007**, *104*, 332-340.

(8) Guo, H.; Zhao, H.; Kanno, Y.; Li, W.; Mu, Y.; Kuang, X.; Inouye, Y.; Koike, K.; Jiang, H.; Bai, H. A dihydrochalcone and several homoisoflavonoids from *Polygonatum odoratum* are activators of adenosine monophosphate-activated protein kinase. *Bioorg. Med. Chem. Lett.* **2013**, *23*, 3137-3139.

(9) Bai, H.; Li, W.; Zhao, H.; Anzai, Y.; Li, H.; Guo, H.; Kato F.; Koike, K. Isolation and structural elucidation of novel cholestane glycosides and spirostane saponins from *Polygonatum odoratum*. *Steroids* **2014**, *80*, 7-14.

(10) Meng, Z. Y.; Xu, S. X.; Li, W.; Sha, Y. New saponins from *Anemarrhena asphodeloides* Bge. *Zhongguo Yaowu Huaxue Zazhi* **1999**, *9*, 294-298.

(11) Bogacheva, N. G.; Sheichenko, V. I.; Kogan, L. M. Structure of yamogenin tetroside from *Trigonella foenum-graecum* seeds, *Khimiko-Farmatsevticheskii Zhurnal* **1977**, *11*, 65-69.

(12) Son, K. H.; Do, J. C.; Kang, S. S. Steroidal saponins from the rhizomes of *Polygonatum sibiricum*. *J. Nat. Prod*. **1990**, *53*, 333-339.

(13) Sugiyama, M.; Nakano, K.; Tomimatsu, T.; Nohara, T. Five steroidal components from the rhizomes of *Polygonatum odoratum* var. *pluriflorum*. *Chem. Pharm. Bull.* **1984**, *32*, 1365-1372.

(14) Mimaki, Y.; Kuroda, M.; Fukasawa, T.; Sashida, Y. Steroidal glycosides from the bulbs of *Allium jesdianum*. *J. Nat. Prod*. **1999**, *62*, 194-197.

(15) Braca, A.; Prieto, J. M.; De Tommasi, N.; Tomè, F.; Morelli, I. Furostanol saponins and quercetin glycosides from the leaves of *Helleborus viridis* L. *Phytochemistry* **2004**, *65*, 2921-2928.

(16) Agrawal, P. K. Dependence of ^{1}H NMR chemical shifts of geminal protons of glycosyloxy methylene (H_2-26) on the orientation of the 27-methyl group of furostane-type steroidal saponins. *Magn. Reson. Chem.* **2004**, *42*, 990-993.

(17) Yu, G. F.; Mulabagal, V.; Diyabalanage, T.; Hurtada, W. A.; DeWitt, D. L.; Nair, M. G.

Non-nutritive functional agents in rattan-shoots, a food consumed by native people in the Philippines. *Food Chem.* **2008**, *110*, 991-996.

(18) Liu, Z. H.; Yan, H.; Si, Y. A.; Ni, W.; Chen, Y.; He, L.; Liu, H. Y. Bioactive spirostane glycosides from *Tacca plantaginea*. *Steroids* **2016**, *106*, 86-92.

(19) Li, C.; Chen, J.; Lu, B.; Shi, Z.; Wang, H.; Zhang, B.; Zhao, K., Qi, W.; Bao, J.; Wang, Y. Molecular switch role of Akt in *Polygonatum odoratum* lectin-induced apoptosis and autophagy in human non-small cell lung cancer A549 cells. *PloS one* **2014**, *9*, e101526.

(20) Zhonghuabencao Editorial Board, Zhonghuabencao. Shanghai Scientific and Technological Press, Shanghai, **1999**, *Vol. 8*, pp. 7198-7200.

Figure legends

Figure 1. Key HMBC and DQFCOSY correlations of **1** and **2**.

Figure 2. Key ROESY correlations of the aglycone part in **1**.

Figure 3. ESI-MS spectra of **1-8** in positive-ion mode. (a) (+) ESI-MS spectrum of **1**; (b) (+) ESI-MS spectrum of **2**; (c) (+) ESI-MS spectrum of **3**; (d) (+) ESI-MS spectrum of **4**; (e) (+) ESI-MS spectrum of compound **5**; (f) (+) ESI-MS spectrum of compound **6**; (g) (+) ESI-MS spectrum of **7**; (h) (+) ESI-MS spectrum of **8**.

Figure 4. Proposed fragmentation pathways and characteristic ions of **1**, **3**, **5** and **7** in positive-ion mode. (a) Proposed fragmentation pathway for **1**; (b) Proposed fragmentation pathway for **3**; (c) Proposed fragmentation pathway for **5**; (d) Proposed fragmentation pathway for **7**.

Figure 5. Total ion chromatograms of the crude extract from *P. odoratum* rhizomes (Anhui Cultivar; Nov. 2014). (a) (+) ESI-MS spectrum; (b) (-) ESI-MS spectrum. (c-g) Selected ion monitoring chromatogram of *m/z* 593, 395, 577, 415 and 399.

Figure 6. Contents of steroidal glycosides in cultivated *P. odoratum* rhizomes from Anhui province which were collected from April 2015 to June 2017.

Figure 7. Possible biosynthetic pathway for **1-8**.

Table 1. NMR spectroscopic data (500 MHz for ^{1}H and 125 MHz for ^{13}C, in pyridine-d_5) of compounds 1 and 2

no.	1		2		no.	1		2	
	δ_C	δ_H	δ_C	δ_H		δ_C	δ_H	δ_C	δ_H
aglycone					sugar				
1	37.8	1.72, m	38.0	1.86[a]	3-*O*-sugar				
		1.00[a]		1.17, dd (13.7, 3.7)	β-D-Gal				
2	30.2	2.06, m	32.1	2.30, dd (12.3, 7.4)	1	102.8	4.83, d (7.5)		
		1.74, m		1.52, dt (12.3, 3.2)	2	73.2	4.38, t (8.8)		
3	78.3	3.90, m	71.3	3.79, m	3	75.6	4.03, dd (8.8, 3.4)		
4	39.3	2.64, dd (13.2, 2.6)	43.2	2.62, 2H, brd (6.9)	4	79.8	4.54, brd (3.4)		
		2.46, t (13.2)			5	75.2	3.91, m		
5	140.6		141.5		6	60.6	4.61[a]		
6	122.2	5.36[a]	121.6	5.47, brd (3.4)			4.11[a]		
7	26.7	2.46, t (13.2)	26.7	2.52, dd (17.2, 10.6)	β-D-Glc1				
		1.83, dd (13.2, 6.3)		1.93, m	1	105.0	5.13, d (8.1)		
8	35.6	2.03, m	35.7	2.13, dd (10.6, 5.5)	2	81.3	4.35, dd (8.3, 8.1)		
9	43.7	1.79, m	43.8	1.88, m	3	86.9	4.13, t (8.8)		
10	37.4		37.4		4	70.5	3.79, dd (9.5, 8.8)		
11	20.4	1.55, 2H, m	20.5	1.62, 2H, brdd (9.2, 3.4)	5	77.6	3.82, ddd (9.5, 5.2, 2.0)		
12	32.0	2.27, dd (12.6, 7.5)	32.7	2.07, dd (12.9, 4.0)	6	62.9	4.48, dd (10.3, 2.0)		
		1.49, t (12.6)		1.78, brd (12.9)			4.35[a]		
13	45.4		45.4		β-D-Glc2				
14	86.4		86.4		1	104.8	5.53, d (7.7)		
15	40.1	2.27, dd (12.6, 7.5)	40.1	2.30, dd (12.6, 7.4)	2	76.2	4.03, t (8.7)		
		1.85, dd (12.6, 6.0)		1.87, dd (12.6, 6.0)	3	77.8	4.07[a]		
16	81.8	5.37[a]	81.8	5.40, dd (13.7, 7.4)	4	71.1	4.13, t (8.8)		
17	60.6	2.86, dd (8.1, 6.3)	60.6	2.88, dd (8.0, 6.5)	5	78.6	3.87, ddd (8.6, 5.2, 2.3)		
18	20.1	1.10, s	20.2	1.14, s	6	62.9	4.52, dd (11.4, 2.3)		
19	19.3	0.98, s	19.5	1.13, s			4.34, dd (11.4, 5.2)		
20	40.8	2.34, qui (6.9)	40.8	2.37, t (6.9)	β-D-xyl				
21	16.6	1.32, d (6.9)	16.7	1.34, d (6.9)	1	104.9	5.20, d (7.7)		
22	111.0		111.0		2	75.1	3.91[a]		
23	37.2	2.08, m	37.2	2.08, m	3	78.6	4.03, t (8.6)		
		1.99, m		1.98, m	4	70.7	4.08, m		
24	28.3	2.06, m	28.4	2.07, m	5	67.2	4.21, dd (11.2, 5.1)		
		1.72, m		1.73, m			3.64, t (11.2)		
25	34.5	1.93, m	34.5	1.94, m	26-*O*-sugar				
26	75.4	4.07[a]	75.4	4.09, dd (9.4, 5.8)	β-D-Glc3			β-D-Glc	
		3.50, dd (9.5, 6.9)		3.51, dd (9.4, 6.8)	1	105.1	4.79, d (7.7)	105.1	4.79, d (7.7)
27	17.5	1.04, d (6.5)	17.5	1.05, d (6.6)	2	75.3	3.97, t (8.0)	75.2	3.98, t (8.3)
					3	78.6	4.19[a]	78.6	4.19[a]
					4	71.8	4.18, m	71.7	4.18, m
					5	78.5	3.91, m	78.4	3.90, ddd (9.4, 5.2, 2.3)
					6	62.5	4.49, dd (11.5, 2.0)	60.6	4.50, dd (11.7, 2.3)
							4.35, dd (11.5, 5.2)		4.34, dd (11.7, 5.2)

[a]Overlapped with other signals.

Table 2. Steroidal glycosides in cultivated and wild *P. odoratum* from different collecting date and origins (mg/g dry weight)

Origin	Samples	Collecting date	**1**	**2**	**3**	**4**	**5**	**6**	**7**	**8**	Total
Anhui Cultivar	PO201504	Apr. 15, 2015	3.291	0.043	1.388	-	1.284	0.028	5.273	0.320	11.627
	PO201505	May. 15, 2015	4.651	0.315	1.171	0.007	1.604	0.042	3.691	0.360	11.840
	PO201507	Jul. 15, 2015	2.519	0.139	0.975	0.005	2.042	0.075	3.345	0.214	9.314
	PO201508	Aug. 15, 2015	2.116	0.096	0.910	0.001	1.311	0.074	5.362	0.238	10.107
	PO201509	Sep. 15, 2015	2.242	0.101	0.755	0.002	0.888	0.053	2.760	0.147	6.947
	PO201510	Oct. 15, 2015	4.238	0.043	0.870	0.005	1.060	0.051	5.799	0.045	12.112
	PO201511	Nov. 15, 2015	3.204	0.016	0.923	-	0.195	0.028	3.141	0.015	7.520
	PO201512	Dec. 15, 2015	2.280	0.029	0.788	-	0.107	0.004	3.300	0.107	6.615
	PO201603	Mar. 15, 2016	4.045	0.075	0.885	0.001	1.235	0.077	4.783	0.280	11.381
	PO201604	Apr. 15, 2016	4.568	0.091	1.944	-	0.920	0.073	7.362	0.295	15.255
	PO201605	May. 15, 2016	3.236	0.000	0.860	0.003	0.359	0.019	5.662	0.187	10.327
	PO201606	Jun. 15, 2016	1.252	0.014	0.197	0.001	0.889	0.041	2.564	0.089	5.032
	PO201607	Jul. 15, 2016	3.917	0.002	0.612	-	0.319	0.023	2.508	0.177	7.559
	PO201608	Aug. 15, 2016	3.388	-	0.837	-	0.726	0.040	1.900	0.171	7.062
	PO201609	Sep. 15, 2016	3.412	0.020	0.955	0.001	0.573	0.067	5.946	0.230	11.183
	PO201611	Nov. 15, 2016	2.590	0.001	0.367	-	0.333	0.014	3.225	0.082	6.612
	PO201612	Dec. 15, 2016	3.626	0.002	0.417	-	0.341	0.011	3.632	0.075	8.103
	PO201701	Jan. 15, 2017	2.878	-	0.558	-	1.693	0.086	4.747	0.250	10.211
	PO201702	Feb. 15, 2017	3.716	-	0.371	-	0.790	0.020	3.547	0.175	8.619
	PO201703	Mar. 15, 2017	4.381	-	0.886	-	1.192	0.163	4.390	0.207	11.220
	PO201704	Apr. 15, 2017	4.568	-	1.944	-	0.920	0.085	7.362	0.295	15.176
	PO201705	May. 15, 2017	3.739	-	0.382	-	1.123	0.029	3.900	0.193	9.366
	PO201706	Jun. 15, 2017	2.689	0.376	0.318	-	1.326	0.325	5.461	0.018	10.136
Hunan Cultivar	POh201608	Aug. 2016	0.396	0.033	0.283	0.001	0.199	0.096	0.301	0.021	1.330
Liaoning Cultivar	POl201608	Aug. 2016	0.353	0.004	0.168	-	0.269	0.008	0.433	-	1.231
Anhui Wild	POw201706	Jun. 2017	2.922	0.002	0.574	-	0.413	0.017	1.553	0.205	5.481

-: Not detected.

Figure 1.

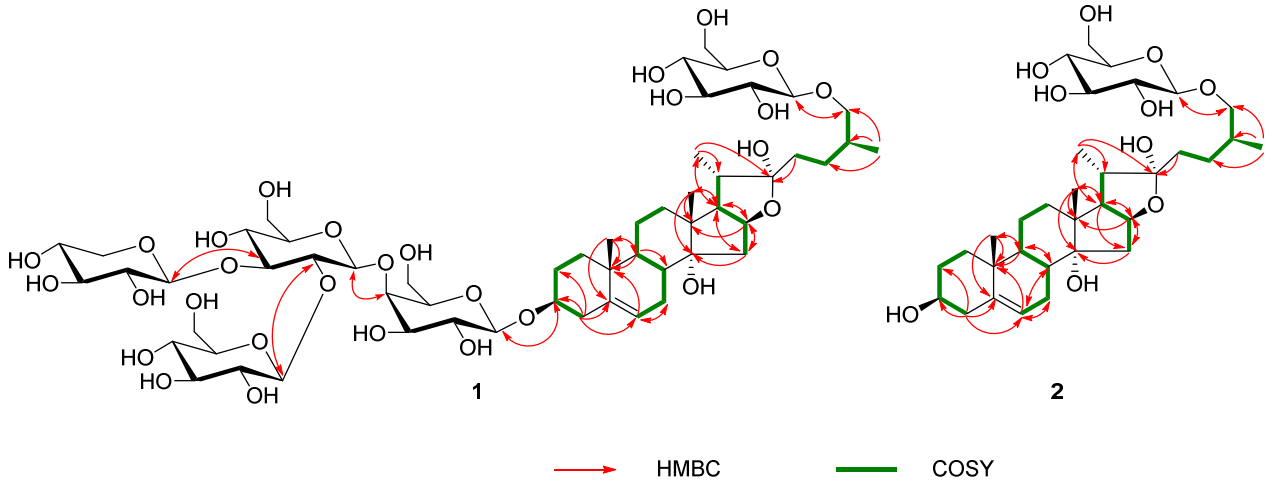

Figure 2.

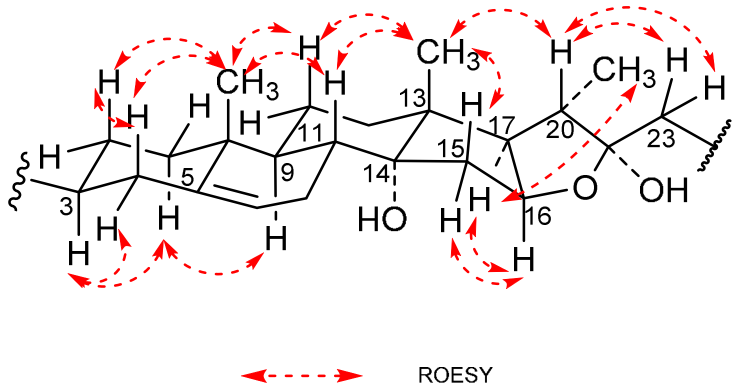

Figure 3.

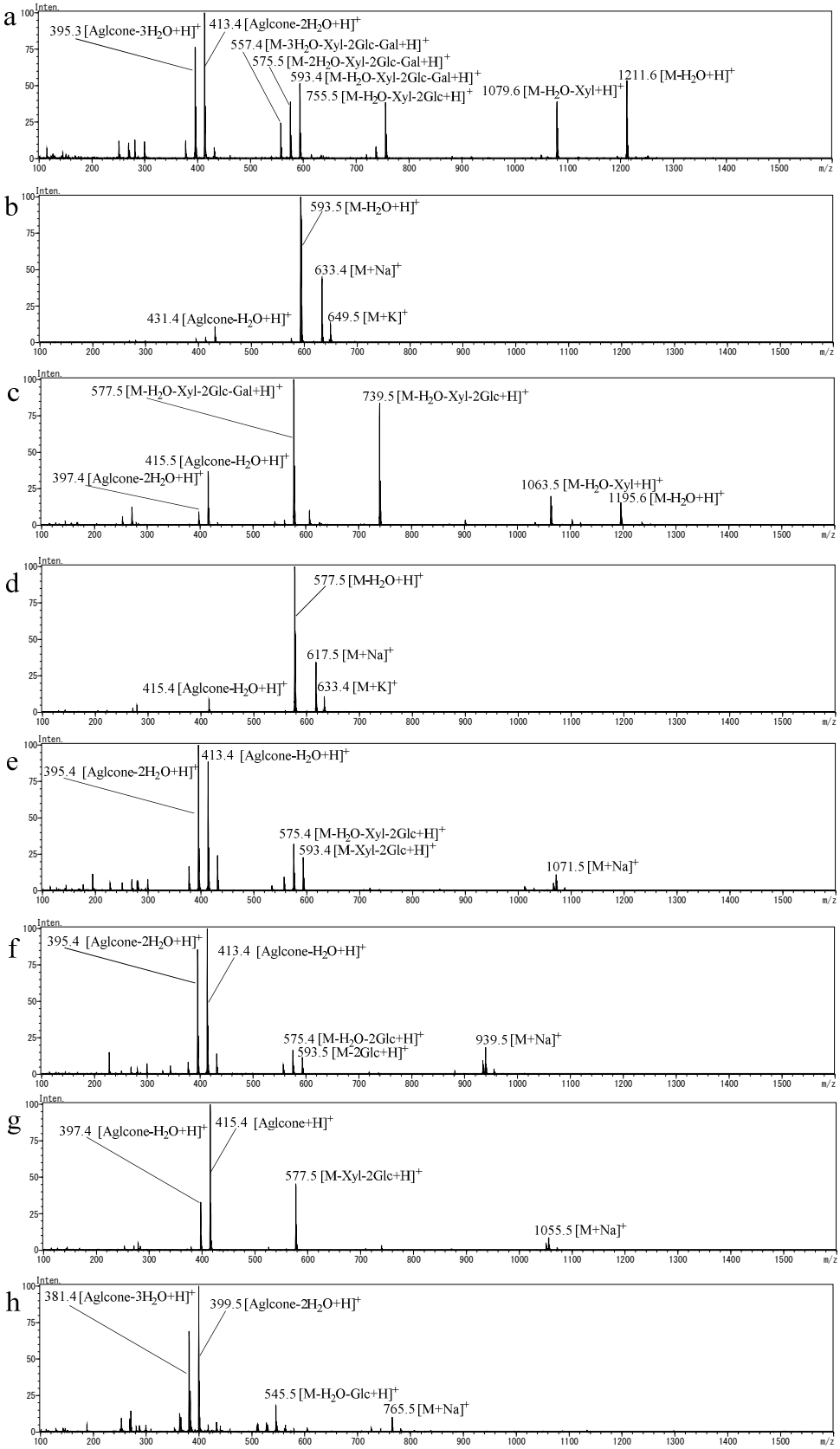
a
395.3 [Aglcone-3H2O+H]+
413.4 [Aglcone-2H2O+H]+
557.4 [M-3H2O-Xyl-2Glc-Gal+H]+
575.5 [M-2H2O-Xyl-2Glc-Gal+H]+
593.4 [M-H2O-Xyl-2Glc-Gal+H]+
755.5 [M-H2O-Xyl-2Glc+H]+
1079.6 [M-H2O-Xyl+H]+
1211.6 [M-H2O+H]+
b
593.5 [M-H2O+H]+
633.4 [M+Na]+
431.4 [Aglcone-H2O+H]+
649.5 [M+K]+
c
577.5 [M-H2O-Xyl-2Glc-Gal+H]+
739.5 [M-H2O-Xyl-2Glc+H]+
415.5 [Aglcone-H2O+H]+
397.4 [Aglcone-2H2O+H]+
1063.5 [M-H2O-Xyl+H]+
1195.6 [M-H2O+H]+
d
577.5 [M-H2O+H]+
617.5 [M+Na]+
415.4 [Aglcone-H2O+H]+
633.4 [M+K]+
e
413.4 [Aglcone-H2O+H]+
395.4 [Aglcone-2H2O+H]+
575.4 [M-H2O-Xyl-2Glc+H]+
593.4 [M-Xyl-2Glc+H]+
1071.5 [M+Na]+
f
395.4 [Aglcone-2H2O+H]+
413.4 [Aglcone-H2O+H]+
575.4 [M-H2O-2Glc+H]+
593.5 [M-2Glc+H]+
939.5 [M+Na]+
g
397.4 [Aglcone-H2O+H]+
415.4 [Aglcone+H]+
577.5 [M-Xyl-2Glc+H]+
1055.5 [M+Na]+
h
381.4 [Aglcone-3H2O+H]+
399.5 [Aglcone-2H2O+H]+
545.5 [M-H2O-Glc+H]+
765.5 [M+Na]+
Inten.
m/z

Figure 4.

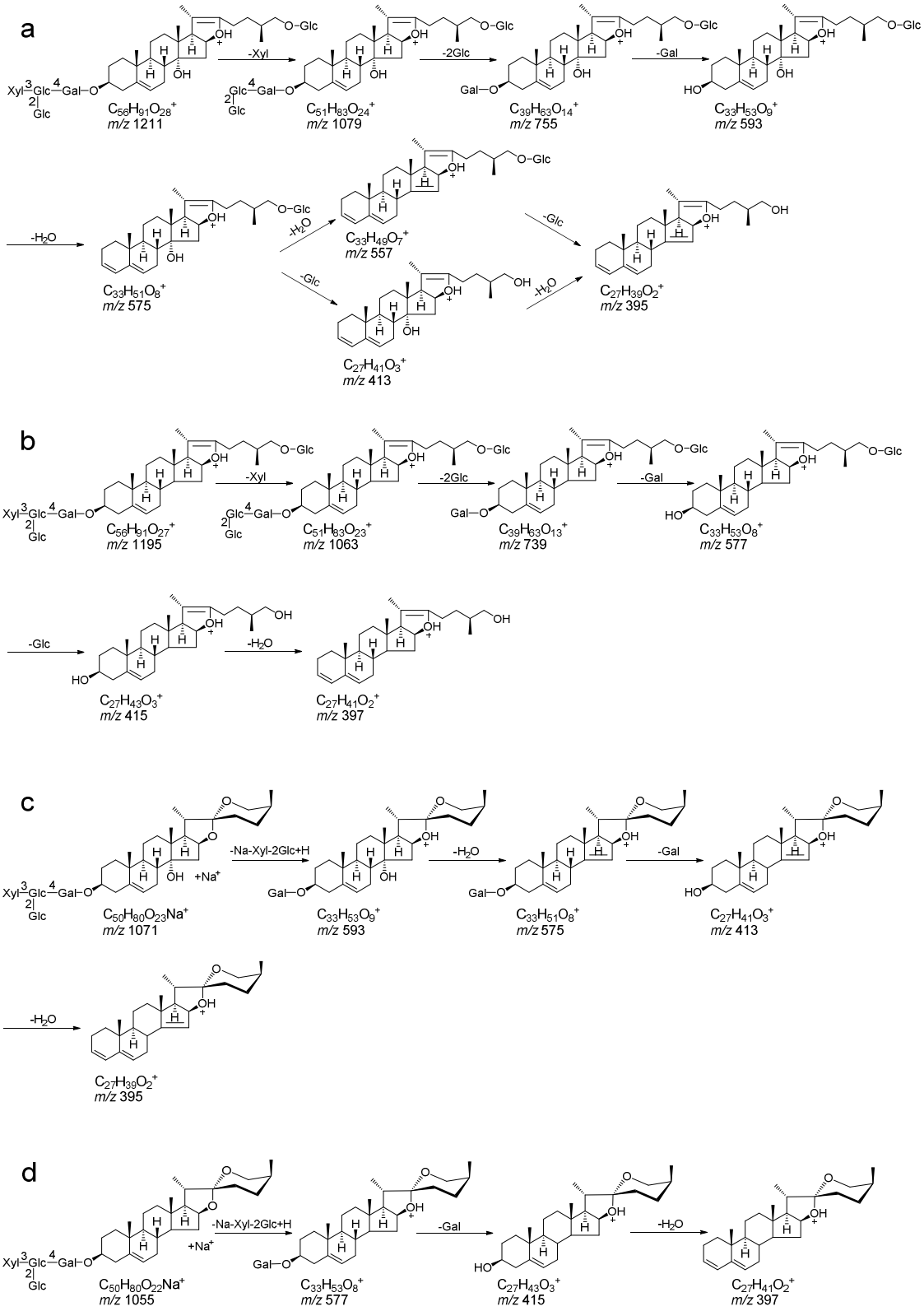
a
-Xyl
-2Glc
-Gal
-H2O
-Glc
C56H91O28+ m/z 1211
C51H83O24+ m/z 1079
C39H63O14+ m/z 755
C33H53O9+ m/z 593
C33H51O8+ m/z 575
C33H49O7+ m/z 557
C27H39O2+ m/z 395
C27H41O3+ m/z 413
b
-Xyl
-2Glc
-Gal
-Glc
-H2O
C56H91O27+ m/z 1195
C51H83O23+ m/z 1063
C39H63O13+ m/z 739
C33H53O8+ m/z 577
C27H43O3+ m/z 415
C27H41O2+ m/z 397
c
-Na-Xyl-2Glc+H
-H2O
-Gal
+Na+
C50H80O23Na+ m/z 1071
C33H53O9+ m/z 593
C33H51O8+ m/z 575
C27H41O3+ m/z 413
C27H39O2+ m/z 395
d
-Na-Xyl-2Glc+H
-Gal
-H2O
+Na+
C50H80O22Na+ m/z 1055
C33H53O8+ m/z 577
C27H43O3+ m/z 415
C27H41O2+ m/z 397

Figure 5.

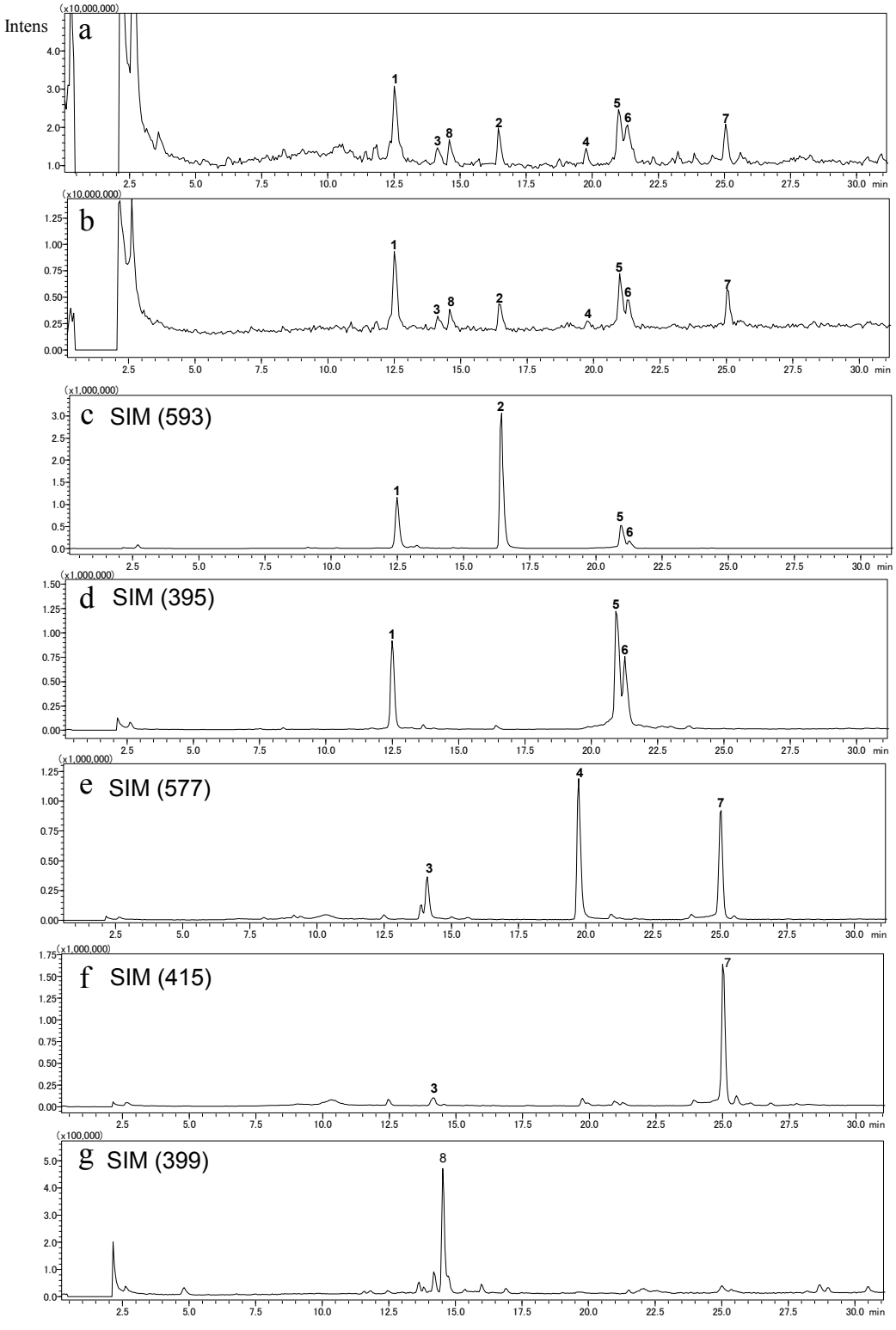
Intens
a
b
c SIM (593)
d SIM (395)
e SIM (577)
f SIM (415)
g SIM (399)
Time (min)

Figure 6.

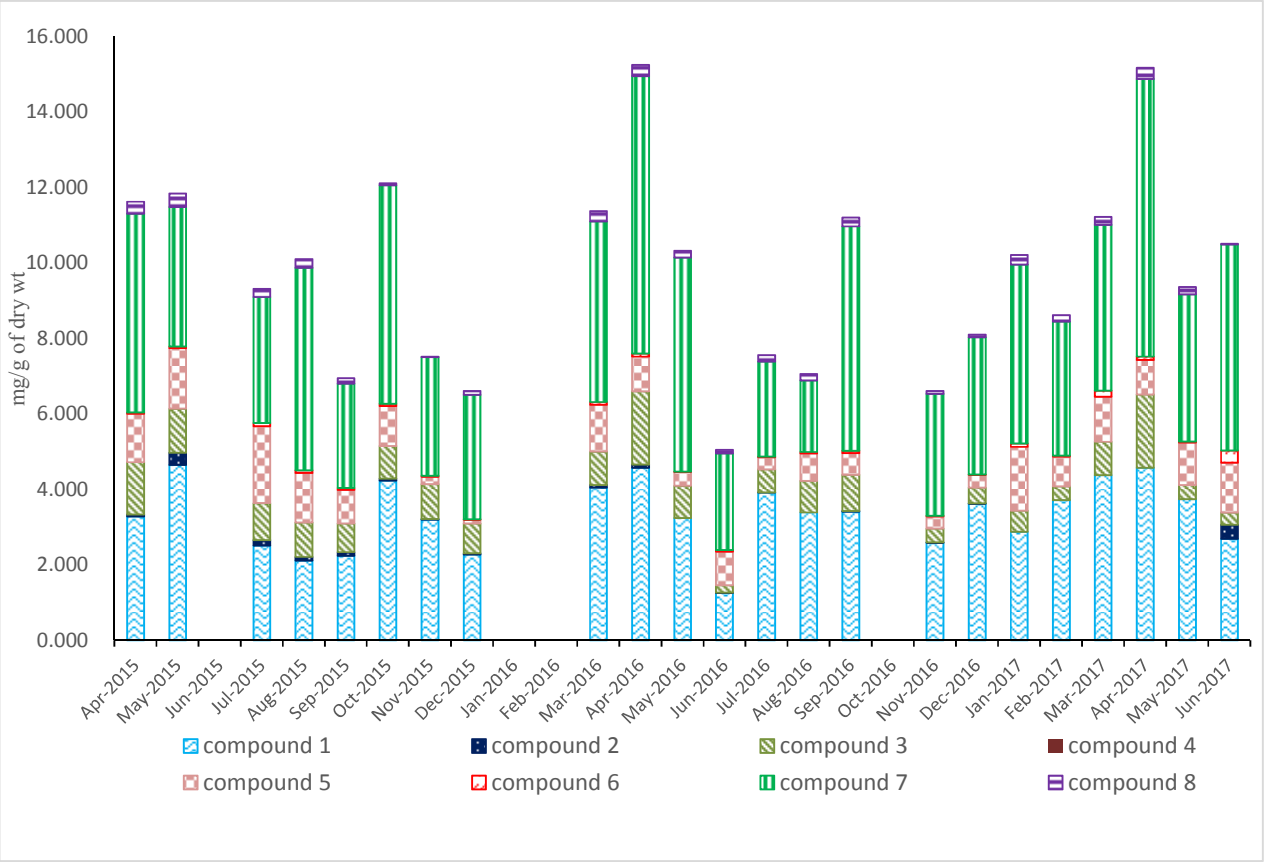
16.000
14.000
12.000
10.000
8.000
6.000
4.000
2.000
0.000
mg/g of dry wt
Apr-2015
May-2015
Jun-2015
Jul-2015
Aug-2015
Sep-2015
Oct-2015
Nov-2015
Dec-2015
Jan-2016
Feb-2016
Mar-2016
Apr-2016
May-2016
Jun-2016
Jul-2016
Aug-2016
Sep-2016
Oct-2016
Nov-2016
Dec-2016
Jan-2017
Feb-2017
Mar-2017
Apr-2017
May-2017
Jun-2017
compound 1
compound 2
compound 3
compound 4
compound 5
compound 6
compound 7
compound 8

Figure 7.

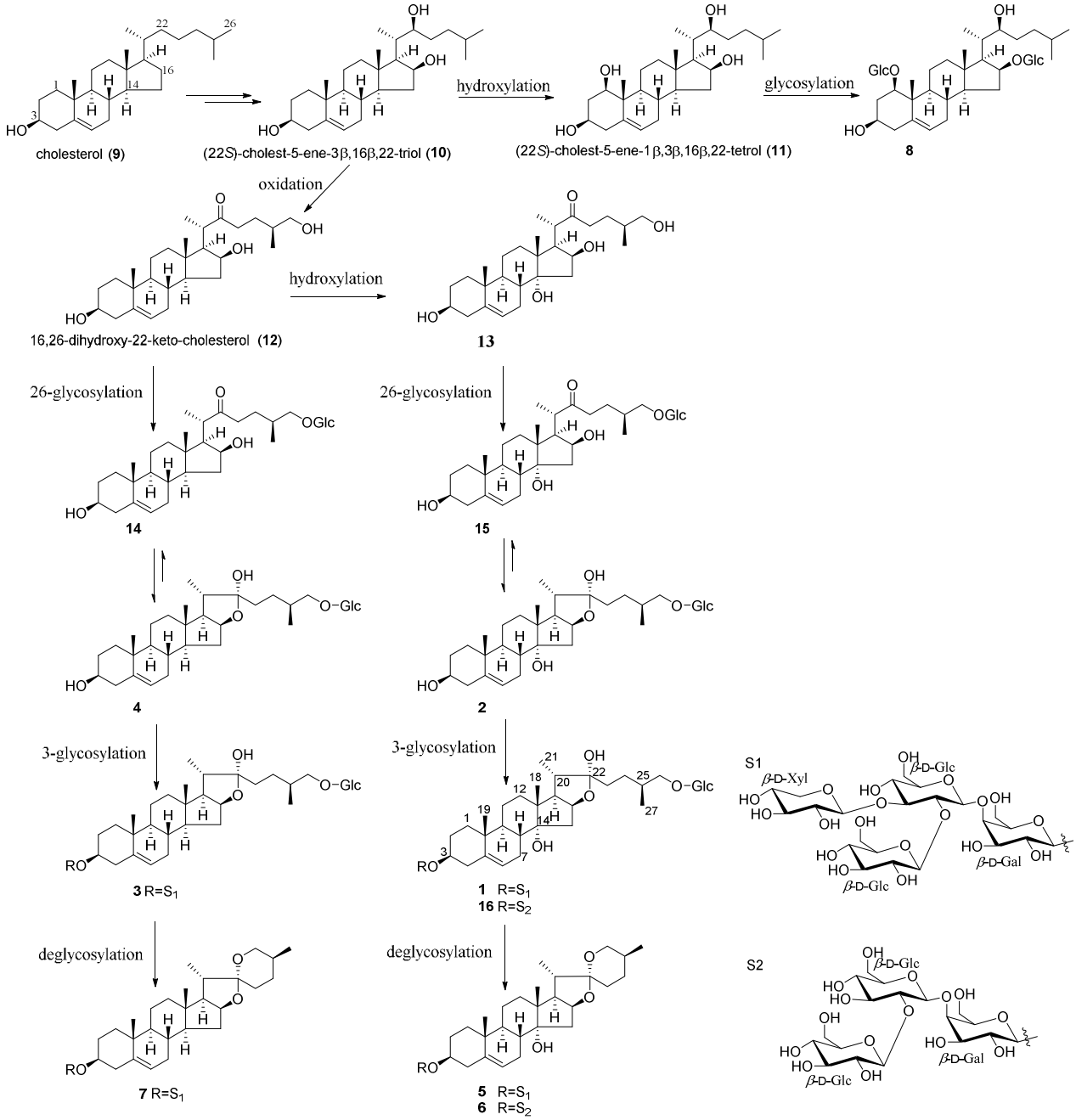
cholesterol (9)
(22S)-cholest-5-ene-3β,16β,22-triol (10)
hydroxylation
(22S)-cholest-5-ene-1β,3β,16β,22-tetrol (11)
glycosylation
8
oxidation
16,26-dihydroxy-22-keto-cholesterol (12)
hydroxylation
13
26-glycosylation
14
26-glycosylation
15
4
2
3-glycosylation
3-glycosylation
3 R=S1
1 R=S1
16 R=S2
deglycosylation
deglycosylation
7 R=S1
5 R=S1
6 R=S2
S1
S2

TOC graphics